

Sources and Processes Affecting Sulfate in a Karstic Groundwater System of the Franconian Alb, Southern Germany

FLORIAN EINSIEDL^{*,†} AND
BERNHARD MAYER[‡]

Institute of Groundwater Ecology, GSF-National Research Center for Environment and Health, Ingolstädter Landstrasse 1, D-85764 Neuherberg, Germany, and Department of Geology and Geophysics, University of Calgary, Calgary, Alberta, Canada T2N 1N4

Chemical and isotope analyses on groundwater sulfate and ³H measurements on groundwater were used to determine the sulfate sources and sulfur transformation processes in a heterogeneous karst aquifer of the Franconian Alb, southern Germany. Sulfate was found to be derived from atmospheric deposition. Young groundwater was characterized by high sulfate concentrations and $\delta^{34}\text{S}$ values similar to those of recent atmospheric sulfate deposition. However, the $\delta^{18}\text{O}$ values of groundwater SO_4^{2-} were depleted by several per mil with respect to those of atmospheric deposition. This isotopic shift is indicative of mineralization of carbon-bonded S in the vadose zone of the karst system. In groundwater with mean residence times of more than 60 years, a trend of increasing $\delta^{34}\text{S}$ values and $\delta^{18}\text{O}$ values with decreasing sulfate concentrations was observed. This trend could not be solely explained by preindustrial atmospheric sulfate deposition with higher $\delta^{34}\text{S}$ values, and hence, we conclude that bacterial (dissimilatory) sulfate reduction in the porous matrix of the karst aquifer must have occurred. This process has the potential to contribute to long-term biodegradation of contaminants in the porous rock matrix representing the dominant water reservoir of the fissured porous karst aquifer.

Introduction

Since the industrial revolution, increasing amounts of anthropogenic sulfur (S) have been emitted to the atmosphere, although a significant decline in the rates of S deposition was observed across large regions in Europe and North America during the past two decades (1). Current atmospheric deposition of S in industrialized countries is mainly derived from anthropogenic sources (2) and is characterized by $\delta^{34}\text{S}$ values typically between 0‰ and 5‰ (3). Several recent studies of historical archives including alpine ice cores (4) and archived wheat grains (5) have suggested that preindustrial atmospheric S had higher $\delta^{34}\text{S}$ values between 8‰ and 11‰. Also, Edmunds et al. (6) interpreted $\delta^{34}\text{S}$ values near 9‰ for sulfate from the East Midlands aquifer in northern England as indicative for sulfate in Holocene rainfall. Marine emissions (sea-spray-derived

sulfate, dimethyl sulfide), one of the major natural atmospheric sulfur sources, are characterized by $\delta^{34}\text{S}$ values of sulfate between 15‰ and 21‰ (7). Therefore, increasing $\delta^{34}\text{S}$ values are expected with decreasing contributions of anthropogenic S to atmospheric sulfate deposition.

Biogeochemical transformation processes in terrestrial and aquatic ecosystems may alter the isotopic composition of deposited sulfate. Throughout the last five decades, the effect of adsorption/desorption (8–10), immobilization, mineralization (11, 12), sulfide oxidation and bacterial (dissimilatory) sulfate reduction (BSR) (13–15) on the isotopic composition of sulfate in soil horizons, aquifers, and sediments has been intensively investigated. Dissimilatory bacterial SO_4^{2-} reduction was found to be the major process in the S cycle causing isotope fractionation, enriching ³⁴S and ¹⁸O in the remaining sulfate (16, 17) and hence causing trends of increasing $\delta^{34}\text{S}$ and $\delta^{18}\text{O}$ values as sulfate concentrations decrease.

So far, most studies on bacterial (dissimilatory) sulfate reduction using isotope techniques were performed in porous aquifers and marine basins (e.g., refs 13 and 18). Little is known about the microbial process, S turnover, and mixing patterns of S from different sources in heterogeneous karst environments. Bottrell et al. (19) found evidence in a dual-porosity aquifer that bacterial sulfate reduction was restricted to the fissures of a limestone aquifer. Moncaster et al. (20) showed for the same aquifer that autotrophic denitrification occurred and was controlled by pyrite availability near the fissures. Hose et al. (21) characterized the microbial community in a H₂S-rich karst environment and identified biogeochemical processes, while Bottrell et al. (22) suggested an ore mineral weathering source for sulfate in the karst aquifer of the Derbyshire Peak District on the basis of S isotope data.

The objective of this study was to determine the sources and the processes affecting sulfate in oxygen-rich, ³H-dated karst groundwater of the Franconian Alb in southern Germany.

Material and Methods

Study Site. The karst aquifer investigated in this study is located in southern Germany north of the Danube River and stretches from the Nördlinger Ries in the west to the city of Kehlheim in the east (Figure 1). The catchment area is approximately 2000 km². The bedrock is composed of Upper Jurassic carbonates, representing two consecutive cycles of sedimentation with marls on the base overlain by well-bedded limestones. The latter contain reef complexes which have been dolomitized. The bedded limestones have porosities of less than 2%, whereas the reef facies is characterized by a rock matrix porosity ranging from 4% to more than 20%, with an arithmetic mean value of 7% (23).

Groundwater flow velocities are considerably lower in the reef facies than in the bedded facies (24). Seiler et al. (24) and Einsiedl (25) provided evidence for the existence of a double-porosity system in the Franconian Alb karst aquifer. The double-porosity concept, previously described by Maloszewski et al. (26) for fissured rocks, is revealed by artificial tracers with different diffusion coefficients. This concept requires the occurrence of diffusive exchange of artificial or environmental tracers between the immobile water in the porous rock matrix and the more mobile water in the fissures of the aquifer. Diffusion processes between the immobile water of the rock matrix and the more mobile water in the fissures (double-porosity concept) influence the water flow and the pollutant transport in the porous reef facies, resulting

* Corresponding author phone: +49 (0) 89 31872567; fax: +49 (0) 89 31873361; e-mail: einsiedl@gsf.de.

† GSF-National Research Center for Environment and Health.

‡ University of Calgary.

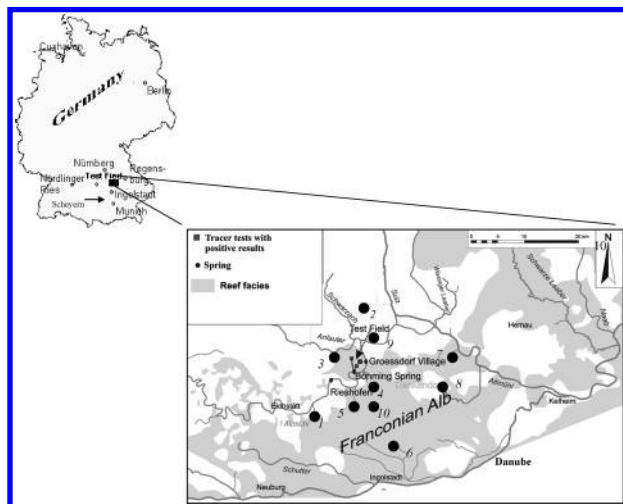


FIGURE 1. 1. Site map of the Franconian Alb karstic catchment area and the investigated springs.

in increasing mean transit times (MTTs) of water and contaminants in the aquifer if matrix diffusion influences the water flow to the springs.

The investigated springs are situated both in the bedded and in the reef facies of the karst aquifer. Annual rainfall is approximately 0.75 m/year. Water balance estimates suggest an annual evapotranspiration of ca. 0.5–0.6 m/year (27). The average air temperature is approximately 8 °C. Groundwater recharge for the Franconian Alb is in the space range of 0.13–0.25 m/year (27, 28).

Sampling. To investigate the S cycle in the karst aquifer of the Franconian Alb, groundwater discharging from 11 springs (site nos. 1–9, Böhming spring, Grössdorf spring) and seepage water of a cave (site no. 10) were sampled (Figure 1). Spring nos. 1 and 4–8 are located in the reef facies, whereas all other springs occur in the bedded facies. Groundwater samples from the 12 sampling sites were obtained up to five times between 2001 and 2004 for chemical and isotope analyses. Atmospheric deposition was sampled repeatedly between February and December of 2001 near the Böhming spring using four rain gauges. Up to 5 L of precipitation water was collected to yield enough sulfate for isotope analyses.

Methods. The standard field measurement program included temperature (°C), electrical conductivity ($\mu\text{S}/\text{cm}$), pH value, alkalinity, and redox potentials (E_h). Water samples obtained from springs for chemical measurements of major cations (Na^+ , K^+ , Ca^{2+} , Mg^{2+}) and anions (Cl^- , SO_4^{2-} , NO_3^-) were 0.45 μm field filtered, collected in 0.5 L plastic bottles, and stored at 5 °C prior to analysis. Standard ion chromatography (Dionex DX 100) was used for determining the concentrations of major cations and anions with an analytical error of less than $\pm 3\%$. Samples for determination of DOC contents were collected in 10 mL glass bottles. DOC contents were determined using a TOC analyzer (TOC 500, Shimadzu Co.) with an analytical error of approximately $\pm 15\%$ at a DOC concentration of about 0.08 mM.

Sulfur and oxygen isotope ratios of sulfate in groundwater and atmospheric deposition were determined. Water samples were acidified to $\text{pH} < 4$ to remove HCO_3^- . Sulfate for isotope analyses was precipitated as BaSO_4 with 5 mL of 0.2 M reagent-grade $\text{BaCl}_2 \cdot 6\text{H}_2\text{O}$ solution. The precipitate was recovered by filtration, carefully washed with distilled water, and dried prior to isotope analyses. Low sulfate concentrations in the rainwater samples required preconcentration of SO_4^{2-} prior to precipitation as BaSO_4 . Up to 5 L of rainwater was passed through an anion-exchange resin (Biorad AG-1X8), and the sulfate was subsequently recovered from the resin with 0.25 L of a 1 M NaCl solution. Thereafter, sulfate

was precipitated as BaSO_4 and purified as described above. Sulfur isotope analyses were performed by isotope ratio mass spectrometry after conversion of BaSO_4 to SO_2 via high-temperature reaction of BaSO_4 with V_2O_5 and SiO_2 (29). For $\delta^{18}\text{O}$ measurements on sulfate, CO_2 and CO were produced through thermal decomposition of BaSO_4 with pure graphite in molybdenum foil under vacuum at more than 1000 °C followed by quantitative conversion of CO to CO_2 in a discharge chamber and subsequent isotope ratio mass spectrometry (30). Water samples for carbon isotope measurements on dissolved inorganic carbon (DIC) were injected into 5 mL of phosphoric acid (96%) in a pre-evacuated flask at 25 °C. The produced CO_2 was purified repeatedly using acetone-dry ice traps and subsequently used for isotope ratio mass spectrometry.

Carbon, sulfur, and oxygen isotope ratios are reported in parts per thousand (‰) using the conventional δ notation:

$$\delta_{\text{sample}} (\text{‰}) = [(R_{\text{sample}} - R_{\text{std}})/R_{\text{std}}] \times 1000 \quad (1)$$

where R_{sample} and R_{std} are the $^{13}\text{C}/^{12}\text{C}$, $^{34}\text{S}/^{32}\text{S}$, or $^{18}\text{O}/^{16}\text{O}$ ratios of the sample and the standard, respectively. $\delta^{34}\text{S}$ values are reported relative to Canon Diablo troilite (V-CDT) and $\delta^{18}\text{O}$ values relative to Vienna standard mean ocean water (V-SMOW). Two international reference materials, NBS-127 and OGS, as well as several laboratory internal standards were repeatedly measured to ensure accuracy. Reproducibility was $\pm 0.2\text{‰}$ for $\delta^{34}\text{S}$ measurements and $\pm 0.5\text{‰}$ for $\delta^{18}\text{O}$ measurements on sulfate. The $^{13}\text{C}/^{12}\text{C}$ ratios of DIC are reported relative to V-PDB with a reproducibility of $\pm 0.2\text{‰}$.

Tritium (^3H) contents were determined for groundwater sampled from the springs in 2003 (site nos. 4–7 and 9, Böhming spring, Grössdorf spring) during base flow conditions. Tritium measurements were conducted by liquid scintillation counting of water after electrolytic enrichment of ^3H (31). The detection limit of this method is 0.7 TU.

Results

Water Chemistry. Table 1 summarizes median values for physical and chemical parameters for groundwater from the karst springs. The karst groundwater was characterized by pH values of 7.1 ± 0.3 and a temperature of ca. 10 °C (cave seepage water pH 8.5, temperature 4 °C, Table 1). Electrical conductivity varied between 555 and 747 $\mu\text{S}/\text{cm}$, and the redox potential ranged between 310 and 157 mV. HCO_3^- concentrations ranged between 5.0 and 6.5 mM (Table 2). All groundwater samples are of the $\text{Ca}^{2+}/\text{Mg}^{2+}-\text{HCO}_3^-$ type characteristic for carbonate aquifers. DOC concentrations in springwater varied between 0.08 and 0.25 mM. Nitrate concentrations ranged from not detectable to 0.75 mM, and chloride concentrations varied between 0.08 and 0.73 mM. In one spring (no. 6) a Cl^- concentration of up to 1.3 mM was observed. Sulfate concentrations varied between 0.08 and 0.36 mM.

Tritium Data. The precipitation record for tritium was obtained from the German precipitation stations at Regensburg (1978–2003), Passau (1970–1977), and Stuttgart (1962–1969) located close to the study area. The ^3H input data were extended backward from 1961 to 1953 using corrected IAEA records from Ottawa and Vienna because no other IAEA stations reported ^3H data prior to 1961.

Tritium contents in groundwater obtained from site nos. 4–7 and 9 and the Grössdorf spring in 2003 ranged from 10.7 to 19.8 TU (Table 3). Additional tritium measurements were conducted for groundwater from the Böhming spring sampled in 1999 and 2001, yielding tritium values of 16.6 and 16.7 TU, respectively. Additional tritium data for samples collected between 1969 (32) and 1980 (33, 27) were also evaluated in this study (Table 3). Tritium contents of up to 182.4 TU were

TABLE 1. Concentrations of Major Dissolved Species in Groundwater Shown as Median Concentrations of the Sampling Intervals between 2001 and 2004

	spring no. 1	s	spring no. 2	s	spring no. 3	s	spring no. 4	s	spring no. 5	s	spring no. 6	s	spring no. 7	s	spring no. 8	s	spring no. 9	s	spring no. 10	Böhming spring	s	Grössdorf spring	s	
pH	7.5		7.4		7.3		7.2		7.8		7.5		7.9		7.8		7.2		8.5		7.1		6.9	
E _h	195		310		169		253		245		252		201		273		187		183		198		176	
[Na ⁺] (mM)	0.23	0.07	0.37	0.02	0.31	0.09	0.33	0.02	0.41	0.10	0.41	0.10	0.29	0.10	0.16	0.0	0.30	0.01	0.08	0.03	0.22	0.03	0.30	0.01
[K ⁺] (mM)	0.02	0.002	2.0	0.05	0.05	0.04	0.05	0.02	0.03	0.02	0.03	0.03	0.04	0.005	0.02	0.0	0.02	0.005	0.01	0.02	0.0	0.07	0.02	
[Ca ²⁺] (mM)	2.02	0.29	3.29	0.23	1.86	0.21	2.49	0.1	1.63	0.42	3.42	0.27	1.87	0.58	1.7	0.13	3.23	0.13	1.24	2.16	2.03	2.03	0.29	
[Mg ²⁺] (mM)	0.95	0.09	0.30	0.12	0.86	0.09	1.14	0.05	0.95	0.23	0.82	0.23	1.05	0.12	0.00	0.05	0.60	0.29	1.62	1.30	1.45	1.45	0.07	
[Cl ⁻] (mM)	0.45	0.03	0.62	0.03	0.62	0.03	0.63	0.03	0.46	0.15	1.28	0.32	0.62	0.07	0.37	0.00	0.44	0.06	0.06	0.46	0.02	0.31	0.02	
[SO ₄ ²⁻] (mM)	0.15	0.03	0.34	0.02	0.24	0.04	0.17	0.00	0.09	0.02	0.16	0.01	0.18	0.01	0.14	0.02	0.33	0.06	0.35	0.20	0.01	0.29	0.03	
[NO ₃ ⁻] (mM)	0.19	0.05	0.77	0.15	0.74	0.08	0.48	0.04	0.06	0.08	0.47	0.02	0.56	0.19	0.35	0.01	0.40	0.03	0.05	0.31	0.01	0.13	0.05	
DOC (mM/C)	0.08		0.08		0.13		0.05		0.25		0.07		0.09		0.09		0.10		0.20		0.09		0.10	

determined for groundwater obtained in 1969 from spring no. 2 located in the bedded facies of the karst aquifer. Throughout the past 30 years tritium contents of approximately 15 TU were consistently found in groundwater at spring nos. 1 and 5, which emerge from the reef facies of the aquifer.

Isotopic Composition of Sulfate and DIC. The $\delta^{34}\text{S}$ values of groundwater sulfate ranged from 1.2‰ to 8.4‰. The $\delta^{18}\text{O}$ values of sulfate varied from 1.5‰ to 13.6‰ (Table 4). The highest $\delta^{34}\text{S}$ value of 8.4‰ in spring no. 5 corresponded with the highest $\delta^{18}\text{O}$ value of sulfate (13.6‰). $\delta^{13}\text{C}$ values of DIC were ca. -13‰ for all samples (Table 2).

The isotopic composition of sulfate in atmospheric deposition sampled between February and December 2001 near Böhming is presented in Table 5. The $\delta^{34}\text{S}$ values ranged from 0.0‰ to 4.9‰. The $\delta^{18}\text{O}$ values in precipitation sulfate varied in the observation period between 8.3‰ in winter and 15.5‰ in summer.

Discussion

Tritium Data and Mathematical Modeling as a Groundwater Dating Tool. The long-term tritium record for precipitation (injection function) and tritium data for groundwater from the 12 sampling sites combined with a simple lumped parameter approach were used to approximate the mean transit time t_p of the tracer and to determine the dispersion parameter P_D (reciprocal of the Peclet number) in the aquifer using a dispersion model. Precipitation water with a known tracer concentration $C_{in}(t)$ infiltrates at the surface of the catchment area and flows through channels with the volumetric flow rate $Q_c(t)$. During very low discharge periods (low-flow condition), the transport of dissolved species in the infiltrated water flowing via sinkholes connected to the conduits (preferential flow) to the springs is practically negligible, and the theoretical tritium concentration for the fissured porous system (low water flow) can be calculated. During low-flow conditions, the water chemistry becomes constant and no significant water component from preferential flow paths mixes with the base flow water. The discharge of the karst springs shows little variability. A dispersion model (eq 2) has to approximate the transit time distribution function of the tracer flow in the fissured porous aquifer (slow water flow) (34).

$$g(\tau) = \frac{1}{\tau \left(4\pi P_D \frac{\tau}{t_p} \right)^{1/2}} \exp \left[\frac{[1 - \tau/t_p]^2}{4 P_D \frac{\tau}{t_p}} \right] \quad (2)$$

The model calibration was performed using the 35 year tritium record for the test field Böhming spring and spring no. 4 (25). The dispersion model applied to the tritium contents observed in the outflow of the springs between 1969 and 2003 at base flow conditions yielded mean transit times t_p of the tracer (Table 3) between 10 years (e.g., no. 9) and more than 100 years (e.g., nos. 1 and 5), and a dispersion parameter of 0.6 for all springs was calculated (Figure 2). From the hydrogeological viewpoint (groundwater recharge, thickness of the aquifer), the long mean transit time of ^3H in the reef facies (with matrix porosity) can only be explained if diffusion processes between fissure water and stagnant matrix water are taken into account. Matrix diffusion is much higher in the reef facies (matrix porosity ca. 7%) as compared to the bedded facies (matrix porosity <2%). This resulted in considerably higher mean transit times for springwater in the reef facies as compared to water from springs in the bedded facies.

Isotopic Composition of Groundwater Sulfate. In Figure 3, sulfate concentrations (a), $\delta^{34}\text{S}$ values (b) and $\delta^{18}\text{O}$ values

TABLE 2. $\delta^{13}\text{C}$ Measurements and HCO_3^- Concentrations in Springwater during June 2003 (Low-Flow Conditions)

	spring no. 1	spring no. 2	spring no. 3	spring no. 4	spring no. 5	spring no. 6	spring no. 7	spring no. 8	spring no. 9	spring no. 10 (cave)	Böhming spring	Grössdorf spring
MTT (years)	150	23		70	120	90	80		10	7–10	62	60
$\delta^{13}\text{C}$ (‰)	–12.3	nd	nd	nd	–12.8	–12.6	–13.5	nd	–12.7	nd	–13.5	–13.5
$[\text{HCO}_3^-]$ (mM)	5.4	5.3	nd	6.2	5.3	5.4	5.3	nd	6.1	5.0	6.5	5.6

TABLE 3. Tritium Contents in Groundwater between 1969 and 2003 during Base Flow (Low Flow) and Calculated MTTs

	spring no. 1	spring no. 2	spring no. 3	spring no. 4	spring no. 5	spring no. 6	spring no. 7	spring no. 8	spring no. 9	spring no. 10	spring no. 11(cave)	Böhming spring	Grössdorf spring
calcd MTT (years)	150	23	—	70	120	90	80	—	10	—	7–10 (estimated)	62	60
^3H (1969) (TU)		182	—	33				—		—		25	
^3H (1980) (TU)	13		—		12			—		—		63	51
^3H (1982) (TU)	16		—	34	7	29	38	—	69	—		56	51
^3H (1983) (TU)	15		—	39	20	30	44	—	69	—		46	58
^3H (1992) (TU)	11		—					—		—		27	33
^3H (1994) (TU)	10		—	18	13	17	18	—	21	—		24	27
^3H (1999) (TU)			—					—		—		17	
^3H (2001) (TU)			—					—		—		17	
^3H (2003) (TU)			—	13	11	12	13	—	14	—		17	20

TABLE 4. $\delta^{34}\text{S}$ and $\delta^{18}\text{O}_{\text{sulfate}}$ Measurements in Springwater from September 2001 to February 2004

	spring no. 1	spring no. 2	spring no. 3	spring no. 4	spring no. 5	spring no. 6	spring no. 7	spring no. 8	spring no. 9	spring no. 10 (cave)	Böhming spring	Grössdorf spring
MTT (years)	150	23		70	120	90	80		10	7–10	62	60
September 2001 (during Groundwater Recharge)												
$\delta^{34}\text{S}$ (‰)	7.4	1.5	2.6	5.4	5.4	6.3	4.9	3.7	1.4	1.3	2.0	1.9
$\delta^{18}\text{O}_{\text{sulfate}}$ (‰)	4.1	3.2	4.2	3.8	3.8	5.8	4.4	5.5	3.3	3.3	3.0	4.9
June 2003 (Low-Flow Conditions)												
$\delta^{34}\text{S}$ (‰)	nd	1.2	3.4	4.8	8.4	7.3	5.8	5.9	2.1	nd	2.0	2.5
$\delta^{18}\text{O}_{\text{sulfate}}$ (‰)	nd	3	3.2	3.6	13.6	4.3	3.4	3.2	2.1	nd	2.7	nd
August 2003 (Low-Flow Conditions)												
$\delta^{34}\text{S}$ (‰)	6.3	1.5	4.5	3.9	6.6	nd	4.9	nd	1.9	nd	2.4	2.0
$\delta^{18}\text{O}_{\text{sulfate}}$ (‰)	3.1	2.3	4.1	2.9	2.5	nd	2.4	nd	1.7	nd	1.7	1.5
January 2004 (Low-Flow Conditions)												
$\delta^{34}\text{S}$ (‰)	nd	nd	3.1	4.4	5.9	nd	nd	nd	2.0	nd	nd	2.2
$\delta^{18}\text{O}_{\text{sulfate}}$ (‰)	nd	2.6	3.0	3.1	3.4	nd	nd	nd	2.3	nd	nd	2.1
February 2004 (Low-Flow Conditions)												
$\delta^{34}\text{S}$ (‰)	7.3	nd	3.3	4.2	6.6	nd	4.6	nd	2.1	nd	2.2	1.7
$\delta^{18}\text{O}_{\text{sulfate}}$ (‰)	3.6	nd	2.6	2.9	5.1	nd	2.5	nd	2.1	nd	1.8	1.5

TABLE 5. Precipitation (mm), Sulfate Concentration (mM), and Isotopic Composition (‰) of Atmospheric Deposition SO_4^{2-}

period	precip	$[\text{SO}_4^{2-}]$	$\delta^{34}\text{S}$	$\delta^{18}\text{O}$
February to April 2001	217	0.033	0.03	8.3
June to August 2001	267	0.036	4.77	15.5
September to October 2001	150	0.041	4.9	12.3
November to December 2001	121	0.038		11.7

(c) of sulfate, and sulfate/chloride ratios (d) are plotted versus the calculated mean transit times. The groundwater samples with the highest mean residence times were characterized by the lowest sulfate concentrations (ca. 0.08 mM). These springs were characterized by $\delta^{34}\text{S}_{\text{sulfate}}$ values around 6.5‰ and $\delta^{18}\text{O}_{\text{sulfate}}$ values between 2.5‰ and 13.6‰ (nos. 1, 5, and 6). In the seepage water of the cave (no. 10) and in karst groundwater from springs with low mean transit times (nos. 2 and 9), SO_4^{2-} concentrations were significantly higher (~0.36 mM) and lower $\delta^{34}\text{S}_{\text{sulfate}}$ values of ca. 1.5‰ and $\delta^{18}\text{O}_{\text{sulfate}}$ values between 1.7‰ and 3.3‰ were observed.

The $\delta^{34}\text{S}$ values for sulfate in groundwater with low mean transit times (nos. 2, 9, and 10) are similar to those of atmospheric sulfate deposition in southern Germany. Sulfate in atmospheric deposition sampled between April and

December 2001 at Böhming (Table 5) had a mean amount-weighted $\delta^{34}\text{S}$ value of 3.3‰. This is consistent with previously reported data from refs 10 and 35 for stations in the vicinity of Munich, indicating that $\delta^{34}\text{S}$ values of sulfate in atmospheric deposition in southern Germany range between 1‰ and 3‰. Therefore, we hypothesize that sulfate in atmospheric deposition is a major source of springwater sulfate. The $\delta^{18}\text{O}$ values of sulfate in the groundwater sampled from the springs, however, were ca. 10‰ lower than those of atmospheric sulfate deposition (amount-weighted mean value, $\delta^{18}\text{O}_{\text{sulfate}} = 12.3$ ‰, Table 5).

Mineralization of Carbon-Bonded S in the Vadose Zone. Since oxygen isotope exchange between H_2O and SO_4^{2-} under environmental conditions proceeds extremely slowly (10^6 to 10^9 years) (36), marked changes of $\delta^{18}\text{O}$ values of sulfate in a flow system are usually caused by SO_4^{2-} reduction and reoxidation. Immobilization of seepage water sulfate in soils and subsequent mineralization of carbon-bonded S have been shown to cause shifts in $\delta^{18}\text{O}$ of SO_4^{2-} (10) similar to those observed in this study. During the formation of mineralized sulfate in the soil zone, four oxygen atoms are incorporated into the newly formed sulfate molecules, with water and atmospheric oxygen constituting the two potential oxygen sources. Using $\delta^{18}\text{O}$ values of –9.5‰ for the incorporated water oxygen (37), enrichment factors $\epsilon = 0.0$ ‰

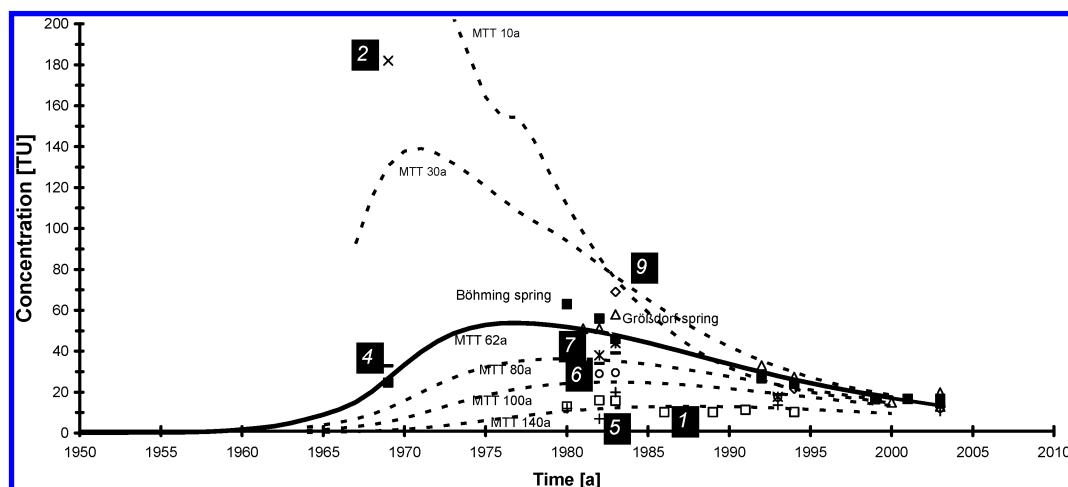


FIGURE 2. Tritium contents in different springs (nos. 1, 2, 4–7, 9, and 11, Böhming and Grössdorf springs) shown as open and closed symbols and theoretical output concentrations using the dispersion model (lines) and calculated MTT in years.

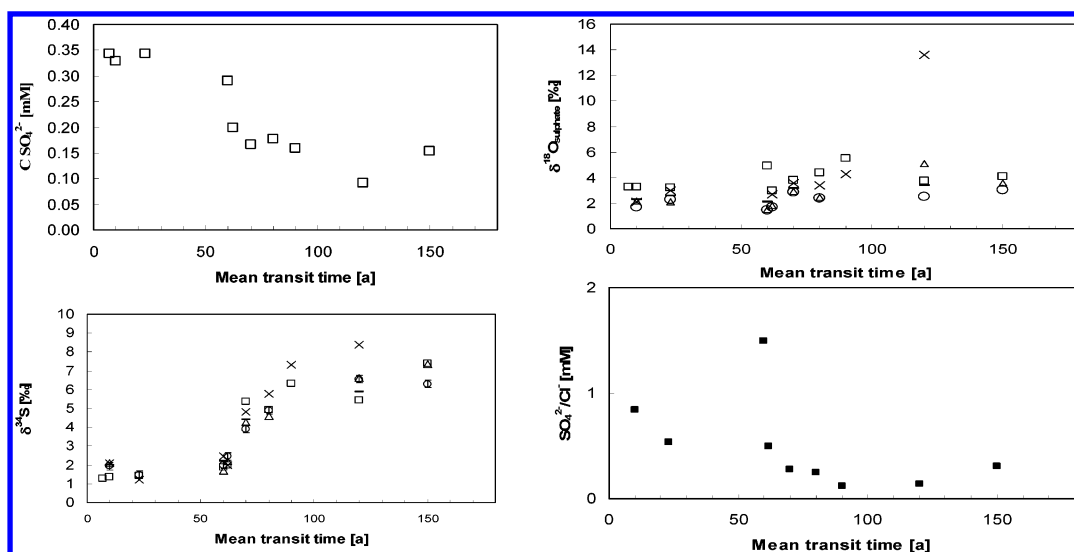


FIGURE 3. (a, top left) Relationship between mean transit time t_p and mean sulfate concentration of groundwater of different karst springs. (b, bottom left) Relationship between MTT and $\delta^{34}\text{S}$ values of sulfate in groundwater from different karst springs in 2001 (squares), June 2003 (times signs), August 2003 (circles), January 2004 (short lines), and February 2004 (triangles). (c, top right) Relationship between mean transit time t_p and $\delta^{18}\text{O}$ values of sulfate in groundwater from different karst springs in 2001 (squares), June 2003 (times signs), August 2003 (circles), January 2004 (short lines), and February 2004 (triangles). (d, bottom right) Relationship between mean transit time t_p and sulfate/chloride ratios in groundwater from different karst springs.

and +4‰ for water oxygen (38, 39) and $\epsilon = -8.7\text{‰}$ for molecular oxygen ($\delta^{18}\text{O} = +23.5\text{‰}$) (40), and an incorporation of 60–70% water oxygen (10, 41), SO_4^{2-} formed by mineralization of carbon-bonded S is expected to have $\delta^{18}\text{O}$ values near 0‰. $\delta^{18}\text{O}$ values of about 2‰ (Figure 3c) and $\delta^{34}\text{S}$ values similar to those of precipitation sulfate (Figure 3b) are consistent with the hypothesis that sulfate in groundwater with mean transit times of less than 30 years is predominantly derived from sulfate in atmospheric deposition, which has undergone at least one immobilization–mineralization cycle in the soil zone before percolating into the groundwater. Sulfate concentrations in springwater with short mean residence times were ca. 7–10 times higher (0.36 mM) than those in recent atmospheric deposition (Table 5). This is consistent with sulfate enrichment due to evapotranspiration (by a factor of 3–6), higher sulfate concentrations in atmospheric deposition until the mid-1980s, and potential contributions from previously stored soil sulfate (1). If sulfate in young groundwater (<30 years) is predominantly derived from atmospheric deposition, the following question arises: Why are sulfate concentrations in older groundwater (>60 years) significantly lower (Figure

3a) and $\delta^{34}\text{S}$ values significantly higher (Figure 3b)? Three potential explanations are discussed below.

Bedrock Sulfate. An explanation for increasing $\delta^{34}\text{S}$ values of sulfate in karst groundwater with mean residence times of >60 years could be sulfate contributions from bedrock weathering. Structurally substituted sulfate in Malm carbonates has $\delta^{34}\text{S}$ values between 15‰ and more than 20‰ (42), while oxygen isotope ratios for Malm sulfate are believed to range between 14‰ and 17‰ (43). If sulfate in older groundwater was increasingly derived from dissolution of carbonate bedrock, this would result in trends of increasing concentrations and $\delta^{34}\text{S}$ and $\delta^{18}\text{O}$ values of sulfate. Since we observed decreasing sulfate concentrations with increasing groundwater age and only minor increases in $\delta^{18}\text{O}_{\text{sulfate}}$ values, it appears that dissolution of bedrock is not a major source of sulfate in the karst groundwater system.

Preindustrial Atmospheric Sulfate Deposition. The calculated mean transit time of water for different springs using a dispersion model represents a flow time distribution, where each stream line represents a flow time of a single tracer particle (τ) (44). Figure 4 shows the portion of different stream lines representing the mean transit times of 60 and

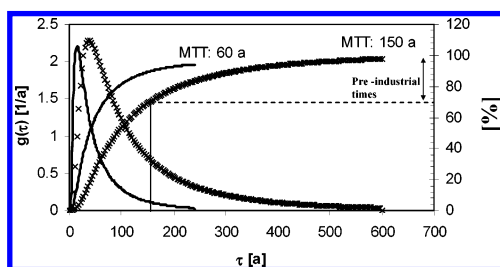


FIGURE 4. Transfer function for a calculated MTT of 60 and 150 years and the portion of preindustrial water (%).

150 years in the groundwater. The modeling results show for groundwater systems representing mean transit times of less than 60 years that flow times τ of water older than 150 years (preindustrial times) are negligible. These groundwater systems are characterized by sulfate with $\delta^{34}\text{S}$ values near 2‰. Groundwater with a mean transit time of 150 years has a portion of ca. 30% of the preindustrial water component, and the $\delta^{34}\text{S}$ values of groundwater sulfate in these waters are ca. 7‰. We tested whether the increase of the $\delta^{34}\text{S}$ values of sulfate in karst groundwater situated in the reef facies (matrix diffusion processes) can be explained by mixing of deposition-derived sulfate of industrial and preindustrial times, with the latter being stored in the porous rock matrix of the reef facies. Mathematical modeling was performed using a $\delta^{34}\text{S}$ value of 3.5‰ (3) for sulfate in atmospheric deposition during industrial times, and sulfate concentrations in atmospheric deposition were markedly lower during preindustrial times compared to those of recent precipitation (45). Assuming that sulfate concentrations in preindustrial atmospheric deposition were more than 50% lower than those in current precipitation, modeled $\delta^{34}\text{S}$ values higher than 21‰ for sulfate in preindustrial precipitation were required to explain the observed $\delta^{34}\text{S}$ values of groundwater sulfate in spring nos. 1 and 5. Since this value is higher than that of sea-salt-derived sulfate, we consider it to be unrealistic for preindustrial atmospheric sulfate deposition. Hence, we conclude that sulfate from preindustrial atmospheric deposition can explain only part of the observed patterns in the chemical and isotopic composition of sulfate in the karst groundwater.

Bacterial (Dissimilatory) Sulfate Reduction. Neither hydrodynamic effects (matrix diffusion processes) nor bed-rock weathering provides a fully satisfactory explanation for the observed trend of decreasing concentrations and increasing $\delta^{34}\text{S}$ values of sulfate in groundwater with mean transit times of >60 years. Therefore, we suggest that BSR is partially responsible for the observed trends of decreasing sulfate concentrations while enriching the remaining sulfate in ^{34}S and ^{18}O (46). In a closed system, isotope fractionation during BSR can be described by the Rayleigh equation:

$$R_t/R_0 = (C/C_0)^{(1/\alpha)-1} \quad (3)$$

R_t and R_0 denote the sulfur isotope ratios of sulfate and C and C_0 represent the concentrations of sulfate at times t and zero, respectively, and α is the isotopic fractionation factor. If the difference between the δ values is small, this equation can be simplified to (36)

$$R_t = R_0 + \epsilon \ln(C/C_0) \quad (4)$$

Plotting the $\delta^{34}\text{S}$ values of groundwater sulfate versus C/C_0 yielded linear trends characteristic for BSR (Figure 5). The isotope fractionation during BSR is commonly quantified in terms of the kinetic fractionation factor α or the isotope enrichment factor ϵ (36). The slope of the linear relationships shown in Figure 5 is equal to ϵ (13). The enrichment factors

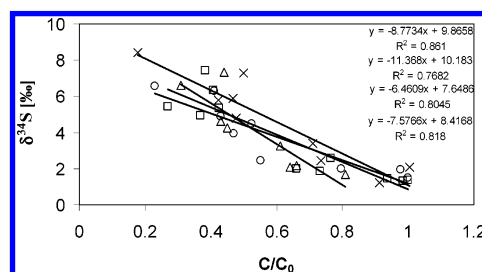


FIGURE 5. $\delta^{34}\text{S}$ as a function of sulfate concentration at times t and zero (C/C_0) for two sampling intervals in 2001 (squares) and 2003 (circles, triangles, times signs).

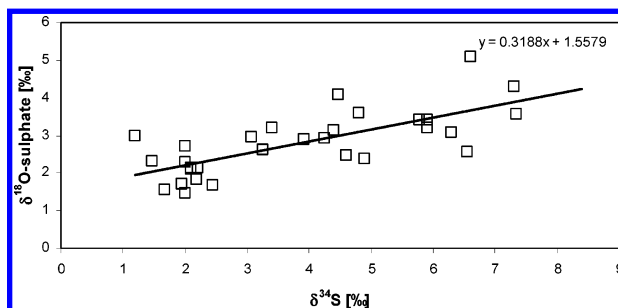


FIGURE 6. Sulfur and oxygen isotope composition of karst water sulfate during base flow conditions in June 2003, August 2003, January 2004, and February 2004.

ϵ determined for data sets from the four sampling events of this study varied between -6.5‰ and -11.4‰ . Similar ϵ values have been reported for other groundwater systems (e.g., ref 13). $\delta^{18}\text{O}$ values of the remaining sulfate are also expected to increase during BSR. Typically, increases in $\delta^{34}\text{S}$ values are up to 4 times higher than those of $\delta^{18}\text{O}$ values in the remaining sulfate during BSR, if fractionation factors are small, reduction rates of sulfate are high, and a limited sulfate supply is assumed (47). Therefore, the increase of the $\delta^{34}\text{S}$ values of ca. 5‰ for sulfate in old groundwater (Figure 3b) was expected to be accompanied by an increase of ca. 1.25‰ in the $\delta^{18}\text{O}_{\text{sulfate}}$ values, if bacterial (dissimilatory) sulfate reduction was the major process responsible for the observed trend. Figure 6 shows that this was indeed the case during low-flow conditions (except for the sampling period in November of 2001) and that the $\delta^{34}\text{S}/\delta^{18}\text{O}$ ratio in the remaining sulfate was in fact close to 4/1. This, together with a decrease in $\text{SO}_4^{2-}/\text{Cl}^-$ ratios (Figure 3d), indicates that BSR provides a suitable explanation for the observed trends in the chemical and isotopic composition of sulfate in the karst groundwater. Additional chemical and isotopic parameters indicative of BSR such as HCO_3^- concentrations and $\delta^{13}\text{C}$ values of DIC proved less informative in our study (Table 2). All groundwater samples had comparatively high HCO_3^- concentrations between 5 and 6.5 mM and $\delta^{13}\text{C}_{\text{DIC}}$ values around -13‰ . Compared to these background values, the expected increase of HCO_3^- concentrations and decrease in $\delta^{13}\text{C}_{\text{DIC}}$ values due to BSR is small and well within the analytical uncertainties of the respective methods and the observed natural variability in HCO_3^- concentrations in springs without BSR. In addition, the presence of sedimentary carbonates of marine ($\delta^{13}\text{C} \approx 0\text{‰}$) and nonmarine origin ($\delta^{13}\text{C} \approx -8\text{‰}$) has been suggested for the Franconian Alb aquifer (48), making carbon isotope ratios of DIC an unreliable indicator for BSR. Indeed, little variation in HCO_3^- concentrations and $\delta^{13}\text{C}_{\text{DIC}}$ values (Table 2) was observed between young and older groundwater, the latter being affected by BSR.

Implications and Environmental Significance

We conclude that sulfate in karstic groundwater of the Franconian Alb in southern Germany is predominantly

derived from atmospheric deposition. Immobilization of deposited sulfate in the vadose zone and remineralization of carbon-bonded S have little influence on the S isotope ratios of sulfate in recharging groundwater but shift its $\delta^{18}\text{O}$ to values significantly lower than those of atmospheric sulfate. Consequently, young groundwater is characterized by relatively high sulfate concentrations and $\delta^{34}\text{S}$ and $\delta^{18}\text{O}$ values around 2‰. Lower sulfate concentrations and elevated $\delta^{34}\text{S}$ values in karstic groundwater with mean residence times of more than 60 years could only partially be explained with potentially higher $^{34}\text{S}/^{32}\text{S}$ ratios in preindustrial atmospheric sulfate deposition. Increasing $\delta^{34}\text{S}$ and $\delta^{18}\text{O}$ values at a ratio close to 4/1 with decreasing sulfate concentrations and $\text{SO}_4^{2-}/\text{Cl}^-$ ratios suggested that bacterial (dissimilatory) sulfate reduction in the rock matrix of the reef facies is partially responsible for the low sulfate concentrations in the older groundwater.

Feast et al. (49) suggested for a similar dual-porosity chalk aquifer in the United Kingdom that elevated sulfate concentrations with “modern” sulfate isotopic composition mix with an older water component in which BSR had occurred presumably in the late Pleistocene. We are unable to judge from our data at which time BSR had occurred in the matrix of the karst groundwater system of the Franconian Alb. However, we point out that there are significant differences in the size of the pore throats in the limestone and chalk aquifer studied by Bottrell et al. (19) and Feast et al. (49) compared to those of the reef facies in our study area. Michel (23) measured pore diameter distributions for the reef facies between 1 and 50 μm and found typical pores with 10 μm in independent laboratory studies. Frederickson et al. (50) found that sulfate-reducing microorganisms range typically from 0.7 to 3 μm in size, indicating the possibility of microbial growth in the porous rock matrix of the reef facies of our study area. In contrast, Bottrell et al. (19) found that pore throats in a chalk and a limestone aquifer in the United Kingdom were too small for growth of microorganisms in the porous rock matrix. Therefore, the presence of a porous rock matrix suitable for microbial growth might enhance the occurrence and affectivity of BSR in the Franconian karst aquifer compared to the aquifer studied by Feast et al. (49) and Bottrell et al. (19).

The karst system of the Franconian Alb represents a double-porosity system that contains rather immobile water in the porous rock matrix and more mobile water in the fissures. The rock matrix is the dominant reservoir for water (25). Heterogeneities of the rock matrix porosity could facilitate anoxic processes (BSR) in the predominantly oxic zone of the karst system. The lack of biodegradation potential in the fissures may explain the presence of nitrate in waters which show evidence of some bacterial sulfate reduction.

Since karst groundwater systems are highly vulnerable to contamination, groundwater protection is a major challenge. There is increasing evidence that anaerobic processes in karst systems with matrix porosity may facilitate biodegradation of contaminants. Some studies have shown (e.g., refs 51 and 52) that, at hydrocarbon-contaminated sites, sulfate-reducing microorganisms contribute extensively to the mineralization of organic contaminants, implying the importance of bacterial sulfate reduction for biodegradation of contaminants (53). Natural attenuation processes including anaerobic microbial degradation of organic contaminants (54–56) could become increasingly important in karst systems with matrix porosity for protecting these groundwater reservoirs as future drinking water resources. The occurrence of nitrate in karst groundwaters with high mean transit times and evidence that BSR had occurred indicate that the limiting factor for biodegradation is probably the separation of electron donor and acceptor in a strong heterogeneous aquifer including matrix diffusion effects.

Literature Cited

- (1) Stoddard, J. L.; Jeffries, D. S.; Lukewille, A.; Clair, T. A.; Dillon, P. J.; Driscoll, C. T.; Forsius, M.; Johannessen, M.; Kahl, J. S.; Kellogg, J. H.; Kemp, A.; Mannio, J.; Monteith, D. T.; Murdoch, P. S.; Patrick, S.; Rebsdorf, A.; Skjelkvale, B. L.; Stainton, M. P.; Traaen, T.; van Dam, H.; Webster, K. E.; Wieting, J.; Wilander, A. Regional trends in aquatic recovery from acidification in North America and Europe. *Nature* **1999**, 401 (6753), 575–578.
- (2) Benkovitz, C.; Schwartz, S. Evaluation of modeled sulfate and SO_2 over North America and Europe for four seasonal months in 1986–1987. *J. Geophys. Res., [Atmos.]* **1997**, 102 (D21), 25305–25338.
- (3) Mayer, B. Potential and Limitation of using Sulphur Isotope Abundance Ratios as an Indicator for Natural and Anthropogenic Environmental Change. *Isotope Techniques in the Study of Environmental Change*; IAEA: Vienna, 1997; pp 423–435.
- (4) Pichlmayer, F.; Blochberger, K. *Stable isotope analysis of sulfur, nitrogen and carbon in glacier snow and aerosol samples*; EUROTRAC Annual Report, 1993, Part 2: ALPTRAC; EUROTRAC International Scientific Secretariat: Garmisch-Partenkirchen, Germany, 1994; pp 43–53.
- (5) Zhao, F. J.; Knights, J. S.; Hu, Z. Y.; McGrath, S. P. Stable sulfur isotope ratio indicates long-term changes in sulfur deposition in the Broadbalk Experiment since 1845. *J. Environ. Qual.* **2003**, 32, 33–39.
- (6) Edmunds, W. M.; Smedley, P. L.; Spiro, B. Controls of the geochemistry of sulphur of the East Midlands Triassic aquifer, UK. *Isot. Water Resour. Manage., Proc. Symp.*, 1995 **1996**, 2, 107–122.
- (7) Nielsen, H. Isotopic composition of the major contributors to the atmospheric sulphur. *Tellus* **1974**, 26, 213–221.
- (8) Stempvoort, D. R. V.; Reardon, E. J.; Fritz, P. Fractionation of sulfur and oxygen isotopes in sulfate by soil sorption. *Geochim. Cosmochim. Acta* **1994**, 54, 2817–2826.
- (9) Stam, A. C.; Mitchell, M. J.; Krouse, H. R.; Kahl, J. S. Stable sulfur isotopes of sulfate in precipitation and stream solutions in a northern hardwood watershed. *Water Resour. Res.* **1992**, 28, 231–236.
- (10) Mayer, B.; Feger, K. H.; Giesemann, A.; Jäger, H. J. Interpretation of sulfur cycling in two catchments in the Black Forest (Germany) using stable sulfur and oxygen isotope data. *Biogeochemistry* **1995**, 30, 31–58.
- (11) Novak, M.; Bottrell, S. H.; Groscheova, H.; F., B.; Cerny, J. Sulfur isotope characteristics of the North Bohemian forest catchments. *Water, Air, Soil Pollut.* **1995**, 85, 1641–1646.
- (12) Michel, R. L.; Campbell, D.; Clow, D.; Turk, J. T. Timescales for migration of atmospherically derived sulphate through an alpine/subalpine watershed, Loch Vale, Colorado. *Water Resour. Res.* **2000**, 36 (1), 27–36.
- (13) Strebel, O.; Böttcher, J.; Fritz, P. Use of isotope fractionation of sulfate-sulfur and sulfate oxygen to assess bacterial desulfurification in a sandy aquifer. *J. Contam. Hydrol.* **1990**, 121, 155–172.
- (14) Alewell, C.; Gehre, M. Patterns of stable S isotopes in a forested catchment as indicators for biological S turnover. *Biogeochemistry* **1999**, 47, 319–333.
- (15) Mandernack, K. W.; Krouse, H. R.; Skei, J. M. A stable sulfur and oxygen isotopic investigation of sulfur cycling in an anoxic marine basin, Frønvare Fjord, Norway. *Chem. Geol.* **2003**, 195, 181–200.
- (16) Kaplan, I. R.; Rittenberger, S. C. Microbiological fractionation of sulfur isotope. *J. Gen. Microbiol.* **1964**, 34, 195–212.
- (17) Canfield, D. E. Isotope fractionation by natural populations of sulfate-reducing bacteria. *Geochim. Cosmochim. Acta* **2001**, 65, 1117–1124.
- (18) Böttcher, M. E.; Khim, B.-K.; Suzuki, A.; Gehre, M.; G., W. U.; Brumsack, H.-J. Microbial sulfate reduction in deep sediments of the Southwest Pacific (ODP Leg 181, Sites 1119–1125): evidence from stable sulfur isotope fractionation and pore water modeling. *Mar. Geol.* **2004**, 205, 249–260.
- (19) Bottrell, S. H.; Moncaster, S. J.; Tellam, J. H.; Lloyd, J. W.; Q. J., F.; Newton, R. J. Controls of bacterial sulphate reduction in a dual porosity aquifer system: the Lincolnshire Limestone aquifer. *Chem. Geol.* **2000**, 169 (3–4), 461–470.
- (20) Moncaster, S. J.; Bottrell, S. H.; Tellam, J. H.; Lloyd, J. W.; Konhauser, K. O. Migration and attenuation of agrochemical pollutants: insights from isotopic analysis of groundwater sulphate. *J. Contam. Hydrol.* **2000**, 43 (2), 147–163.
- (21) Hose, L. D.; Palmer, A. N.; Palmer, M. V.; Northup, D. E.; Boston, P. J.; DuChene, H. R. Microbiology and geochemistry in a hydrogen-sulphide-rich karst environment. *Chem. Geol.* **2000**, 169 (3–4), 399–423.

- (22) Bottrell, S. H.; Webber, N.; Gunn, J.; Worthington, S. The geochemistry of sulphur in a mixed allogenic-autogenic karst catchment, Castleton, Derbyshire, UK. *Earth Surf. Processes Landforms* **2000**, 25, 155–165.
- (23) Michel, U. *Gesteinsphysikalische Eigenschaften und fazielle Ausbildung der oberjurassischen Massenfazies (Kimmeridge) der Südlichen Frankenalb*; GSF Research Center: Neuherberg, Germany, 1999; pp 48–57.
- (24) Seiler, K.-P.; Maloszewski, P.; Behrens, H. Hydrodynamic dispersion in karstified limestones and dolomites in the Upper Jurassic of the Franconian Alb, FRG. *J. Hydrol.* **1989**, 108, 235–247.
- (25) Einsiedl, F. Flow system dynamics and water storage in a fissured-porous karst aquifer. *J. Hydrol.* **2005** (in press).
- (26) Maloszewski, P.; Zuber, A.; Influence of matrix diffusion and exchange reactions on radiocarbon ages in fissured carbonate aquifers. *Water Resour. Res.* **1991**, 27, 1937–1947.
- (27) Pfaff, T. *Grundwasserumsatzräume im Karst der Frankenalb*; GSF Research Center: Neuherberg, Germany, 1987.
- (28) Bavarian Water Management Agency. Grundwasserneubildung in Bayern: Munich, Germany 1996; Vol. 5.
- (29) Yanagisawa, F.; Sakai, H. Precipitation of SO₂ for sulphur isotope ratio measurements by the thermal composition of BaSO₄-V₂O₅-SiO₂ mixtures. *Anal. Chem.* **1983**, 55, 985–987.
- (30) Holt, B. D. *Oxygen isotope*; Wiley: New York, 1991; pp 55–64.
- (31) Eichinger, L.; Forster, M.; Rast, H.; Rauter, W.; Wolf, M. *Experience gathered in low-level measurements of tritium in water*; IAEA: Vienna, 1980; pp 43–64.
- (32) Apel, R. Hydrogeologische Untersuchungen im Malmkarst der südlichen und mittleren Frankenalb. *Geol. Bavarica* **1971**, 64, 268–355.
- (33) Glaser, S. *Der Grundwasserhaushalt in verschiedenen Faziesbereichen des Malmes der Südlichen und Mittleren Frankenalb*; GSF Research Center: Neuherberg, Germany, 1998.
- (34) Maloszewski, P.; Stichler, W.; Zuber, A.; Rank, D. Identifying the flow systems in a karstic-porous aquifer, the Schneetalpe, Austria, by modelling of environmental ¹⁸O und ³H isotopes. *J. Hydrol.* **2002**, 256, 48–59.
- (35) Knief, S. *Isotopenbiogeochemische Untersuchungen über Umsetzungsprozesse des Schwefels in Agrarökosystemen mittels der stabilen Isotope ³⁴S und ¹⁸O*; UFZ Research Center: Leipzig-Halle, Germany, 1998.
- (36) Clark, I.; Fritz, P. *Environmental Isotopes in Hydrogeology*; Lewis Publishers: Boca Raton, FL, 1997.
- (37) Lloyd, R. M. Oxygen-18 composition of oceanic sulfate. *Science* **1967**, 156, 1228–1231.
- (38) Taylor, B. E.; Wheeler, M. C.; Nordstrom, D. K. Stable isotope geochemistry of acid mine drainage. Experimental oxidation of pyrit. *Geochim. Cosmochim. Acta* **1984**, 48, 2669–2678.
- (39) Everdingen, R. O. V.; Shakur, M. A.; Krouse, H. R. Isotope geochemistry of dissolved, precipitated, airborne and fallout sulphur species associated with springs near Paige Mountain, Norman Range. *Can. J. Earth Sci.* **1982**, 19, 1395–1407.
- (40) Devito, K. J.; Fritzgerald, D.; Hill, A. R.; Aravena, R. Nitrate dynamics in relation to lithology and hydrologic flow path in a river riparian zone. *J. Environ. Qual.* **2000**, 29, 1075–1084.
- (41) Toran, I.; Harris, R. F. Interpretation of sulfur and oxygen isotopes in biological and abiological sulfide oxidation. *Geochim. Cosmochim. Acta* **1989**, 53, 2341–2348.
- (42) Kampschulte, A.; Strauss, H. The sulfur isotopic evolution of Phanerozoic seawater based on the analysis of structurally substituted sulfate in carbonates. *Chem. Geol.* **2004**, 204 (3–4), 255–286.
- (43) Pearson, F. J.; Balderer, W.; Loosli, H. H.; Lehmann, B. E.; Matter, A.; Perters, T.; Schmassmann, A.; Gautschi, A. *Applied Isotope Hydrogeology—A case study in Northern Switzerland*; Elsevier: New York, 1991; Vol. 88-01.
- (44) Maloszewski, P. Determining the turnover time of groundwater systems with the aid of environmental tracers, I: Models and their applicability. *J. Hydrol.* **1982**, 57, 207–231.
- (45) Mayewski, P. A.; Lyons, W. B.; Spencer, M. J.; Twickler, M. S.; Buck, C. F.; Whitlow, S. An ice-core record of atmospheric response of anthropogenic sulphate and nitrate. *Nature* **1990** (346), 554–556.
- (46) Harrison, A. G.; Thode, H. G. Mechanism of the bacterial reduction of sulphate from isotope fractionation studies. *Trans. Faraday Soc.* **1958**, 54, 84–92.
- (47) Aharon, P.; Fu, B. Microbial sulfate reduction rates and sulfur and oxygen isotope fractionations at oil and gas seeps in deepwater Gulf of Mexico. *Geochim. Cosmochim. Acta* **2000**, 64 (2), 233–246.
- (48) Prestel, R. Untersuchungen zur Diagenese von Malm-Karbonatgesteinen und Entwicklung des Malm Grundwassers im süddeutschen Molassebecken. Ph.D. Thesis, University of Stuttgart, Stuttgart, Germany, 1990.
- (49) Feast, N. A.; Hiscock, K. M.; Dennis, P. F.; Bottrell, S. H. Controls on stable isotope profiles in the Chalk aquifer of north-east Norfolk, UK, with special reference to dissolved sulphate. *Appl. Geochem.* **1997**, 12, 803–812.
- (50) Frederickson, J. K.; McKinley, J. P.; Bjornstad, B. N.; Long, P. E.; Ringelberg, D. B.; White, D. C.; Krumholz, L. R.; Sufliata, J. M.; Colwell, F. S.; Lehman, R. M.; Phelps, T. J.; Onstott, T. C. Pore-size constraints on the activity and survival of subsurface bacteria in a Late Cretaceous shale-sandstone sequence northwestern New Mexico. *Geomicrobiol. J.* **1997**, 14, 183–202.
- (51) Bolliger, C.; Schroth, M. H.; Bernasconi, S. M.; Kleikemper, J.; Zeyer, J. Sulfur isotope fractionation during microbial sulfate reduction by toluene-degrading bacteria. *Geochim. Cosmochim. Acta* **2001**, 65 (19), 3289–3298.
- (52) Meckenstock, R. U.; Morasch, B.; Griebler, C.; Richnow, H. H. Stable isotope fractionation analysis as a tool to monitor biodegradation in contaminated aquifers. *J. Contam. Hydrol.* **2004**, 75 (3–4), 215–255.
- (53) Ulrich, G. A. B.; G. N.; Cozzarelli, I. M.; Sufliata, J. M. Sources of sulfate supporting anaerobic metabolism in a Contaminated Aquifer. *Environ. Sci. Technol.* **2003**, 37 (6), 1093–1099.
- (54) Kuder, T. W., J. T.; Kaiser, P.; Kolhatkar, R.; Philp, P.; Allen, J. Enrichment of stable carbon and hydrogen isotopes during anaerobic biodegradation of MTBE: Microcosm and field evidence. *Environ. Sci. Technol.* **2005**, 39 (1), 213–220.
- (55) Griebler, C. S., M.; Vieth, A.; Richnow, H. H.; Meckenstock, R. U. Combined application of stable carbon isotope analysis and specific metabolites determination for assessing in situ degradation of aromatic hydrocarbons in a tar oil-contaminated aquifer. *Environ. Sci. Technol.* **2004**, 38 (2), 617–631.
- (56) Rothermich, M. M. H., L. A.; Lovley, D. R. Anaerobic, sulfate-dependent degradation of polycyclic aromatic hydrocarbons in petroleum-contaminated Harbor Sediment. *Environ. Sci. Technol.* **2002**, 36 (22), 4811–4817.

Received for review March 1, 2005. Revised manuscript received July 8, 2005. Accepted July 13, 2005.

ES050426J